Cassette Dosing Approach and Quantitative Structure−Pharmacokinetic Relationship Study of Antifungal *N*-Myristoyltransferase Inhibitors

Kiyoshi Hasegawa,* Hidetoshi Shindoh, Yasuhiko Shiratori, Tatsuo Ohtsuka, Yuko Aoki, Shigeyasu Ichihara, Ikuo Horii, and Nobuo Shimma

Nippon Roche Research Center, 200 Kajiwara, Kamakura, Kanagawa, 247-8530, Japan

Received December 27, 2001

Pharmacokinetic (PK) parameters of *N*-myristoyltransferase (Nmt) inhibitors were measured, and a multivariate quantitative structure−pharmacokinetic relationship (QSPKR) model for predicting rat elimination half-life ($t_{1/2}$) values was constructed. One hundred seven benzofuran derivatives have been selected as the data set for QSPKR analysis. The correlation between the $t_{1/2}$ values and 30 physicochemical descriptors was examined by a stepwise multiple linear regression method. The statistical analysis gives a significant QSPKR model ($r = 0.843$) with the following three variables: partial negative surface area (PNSA), atomic-based octanol/water partition coefficient (AlogP), and the number of rotational bonds (Rotlbonds). The QSPKR model obtained is predictive and simple, and would give a direction for designing new Nmt inhibitors having good PK profiles.

INTRODUCTION

Drug development often fails because of poor pharmacokinetic (PK) properties of the drug candidate. For minimizing the risk of such failure, selection of compounds having good PK properties is required in the early stage of a drug discovery program.[1,2] High-throughput PK measuring methods such as the cassette dosing method[3−9] and sample pooling method[10−12] have been recently developed in the pharmaceutical industry. These methods increase the screening capability in selecting lead compounds and new drug candidates that have good PK properties.

High-throughput PK measurement can pool a large amount of PK data, and thus a good computational prediction model can be constructed. The computational prediction model becomes more useful when PK parameters can be predicted from the molecular structure alone. The model may obviate experimental determinations of PK parameters and even the actual synthesis of compounds with undesired PK properties. Moreover, the model may be used to design favorable compounds based on the selected physicochemical variables. For these beneficial reasons, quantitative structure−pharmacokinetic relationships (QSPKRs) have been developed for several congeneric series of molecules, and various mathematical models have been proposed.[13−15] However, the vast majority of QSPKR studies have focused only on the univariate correlation of individual PK parameters with lipophilicity and the ionization constant of a molecule. A major drawback of such QSPKR models is that they provide no insight into the influence of other physicochemical variables and therefore their predictions are rather limited. Because of these limitations, only a few attempts have been made to develop more comprehensive multivariate QSPKR models based on various molecular physicochemical descriptors.[16,17]

In our *N*-myristoyltransferase (Nmt) inhibitor project[18,19] aiming at the development of a novel antifungal agent for treatment of systemic mycoses, prediction of the PK parameters of designed inhibitors by molecular physicochemical descriptors alone was urged. For predicting rat elimination half-life ($t_{1/2}$) values, we constructed a comprehensive multivariate QSPKR model based on various molecular physicochemical descriptors. The PK parameters were obtained by cassette dosing in a high-throughput manner. In total, 30 physicochemical descriptors were generated for an entire three-dimensional (3D) structure as well as for an individual fragment. The correlation between the $t_{1/2}$ values and the physicochemical descriptors was examined by a stepwise multiple linear regression method. The statistical analysis gave a significant QSPKR model with three variables. The QSPKR model obtained is predictive and simple, and would give a direction for designing new Nmt inhibitors having good PK profiles.

EXPERIMENTAL SECTION

Chemicals. All the inhibitors were synthesized at Nippon Roche Research Center. HPLC-grade methanol, acetonitrile, reagent-grade dimethyl sulfoxide (DMSO), poly(ethylene glycol) 300 (PEG300), formic acid, and ammonium formate were purchased from Wako Pure Chemical Industries, Ltd. (Osaka, Japan). Hydroxypropyl β-cyclodextrin (HPCD) was purchased from Nihon Shokuhin Kako Co., Ltd. (Tokyo, Japan).

PK Experiment. Four-week-old male Fischer rats were purchased from Charles River Japan Inc. (Yokohama, Japan). Rats were housed in individual cages and allowed chow and water ad libitum. Six rats ranging from 55 to 75 g were used in each cassette PK experiment.

Four compounds and one reference compound (**1**) were dissolved individually in DMSO at a concentration of 20 mg/mL. These solutions (60 μL each) and PEG300 (300 μL)

* Corresponding author e-mail: kiyoshi.hasegawa@roche.com.

10.1021/ci0102517 CCC: $22.00 © 2002 American Chemical Society
Published on Web 06/07/2002

were mixed, and then 5.4 mL of 10% aqueous HPCD solution was added to the mixture. The final concentration of each compound was 0.2 mg/mL in 5% DMSO−5% PEG300−10% HPCD solution. Ten mL/kg cocktail solution was administered to rats intravenously at 2 mg/kg for each compound.

Six rats were divided into two groups, A and B (n = 3/group). Approximately 0.5 mL of blood was collected from the retroorbital vein from group A at 10 min and at 1 h and from group B at 30 min and at 2 h after dosing. Blood samples from the heart were collected from group A at 4 h and from group B at 7 h. Heparin was used as an anticoagulant (approximately 10 μL/0.5 mL of blood). Plasma was separated by centrifugation and stored at −40 °C.

One hundred microliters of plasma was precipitated by adding 200 μL of acetonitrile containing 0.2 μg/mL internal standard. After centrifugation, the supernatant was evaporated to dryness under a N_2 gas stream at 37 °C. One hundred microliters of HPLC solvent was added to the residue, and then the mixture was recentrifuged. Twenty to forty microliters of the supernatant was injected into LC/MS/MS. A Develosil C8 column, 5 μm, 4.6 × 50 mm (Nomura Chemical Co., Ltd., Japan), was used as the analytical column. The HPLC mobile phase consisting of 0.1% formic acid in methanol:0.1% formic acid in water = 60:75 to 40:25 (v/v) or methanol:0.1% formic acid and 5 mM ammonium formate in water (approximately pH 3) = 60:75 to 40:25 (v/v). The flow rate was set at 1.0 mL/min and the mobile phase was split after the analytical column. Approximately 20 μL/min sample eluent was flown into an atmospheric pressure ionization (API) mass spectrometer, API-300 (PE Sciex, Concord, NO, Canada). Each analyte was quantified by the multireaction monitoring (MRM) method with a positive ion mode. Data calibration was performed using MacQuan software (MassChrom 1.0, PE Sciex). A calibration curve for each compound in rat plasma was prepared from 10 to 1000 ng/mL. Concentration data were calculated based on the ratio of the peak areas between each compound and the internal standard. Linear regression analysis by a weighting factor of $1/y^2$ was used to fit the calibration curves.

Calculation of PK Parameters. The clearance (Cl), steady-state volume of distribution (V_{ss}), and $t_{1/2}$ of each compound were derived from the respective plasma concentration versus time curve using noncompartmental methods. The area under the plasma concentration curve (AUC) from zero to either the last sampling time or the last time with a measurable concentration was estimated using a trapezoidal method. $C_{10\ \mathrm{min}}$ values were the plasma concentrations at 10 min.

Data Set for QSPKR Study. One hundred seven benzofuran derivatives from two different series were selected as a data set for the QSPKR study. The first series of compounds consists of 83 ether and amide derivatives at the C-2 position of the benzofuran ring. The second series are 24 ketone derivatives at the same position. These series of compounds were synthesized in the course of the NMT inhibitor project, and they showed potent antifungal activity against *Candida albicans*.[18,19] The chemical structures and values of three PK parameters (ln($t_{1/2}$), ln(Cl), ln(V_{ss})) are shown in Tables 1 and 2. The $t_{1/2}$ value was used as the target pharmacokinetic parameter for modeling since it is largely related to in vivo efficacy in rats in the project. Other PK parameters (Cl and V_{ss}), however, showed no significant correlation with the chemical descriptors.

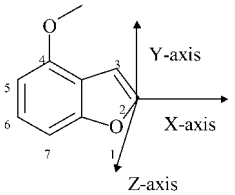

Figure 1. Definition of the Cartesian coordinate system.

Molecular Modeling. Each compound was built up from the fragment library in the Cerius2 program package[22] as an extended conformation and was modeled in the neutral form. Each structure was fully optimized using a molecular mechanics force field with a distance-dependent dielectric function (CVFF force field). We adopted the default minimizer module in Cerius2 that uses a cascade of two minimization algorithms in sequence. The adopted-basis Newton−Raphson algorithm was first used for 10−100 steps, and then the quasi Newton−Raphson algorithm was used to complete the minimization to convergence (0.001 kcal/mol). The partial atomic charges required for energy minimization were assigned using Gasteiger's method. The obtained 3D structures were located in the predefined Cartesian coordinates system (x, y, z) such that the bond from position 2 of the benzofuran ring was aligned with the positive x-axis and the benzofuran ring itself in the $x-y$ plane (Figure 1).

Chemical Descriptors. The superimposed 3D chemical structure was used to compute various chemical descriptors related to the molecular features. Five types of chemical descriptors (electronic, spatial, structural, thermodynamic, and topological) were calculated for the entire structure as well as for individual fragments contributing to the $t_{1/2}$ values. The list of 30 chemical descriptors is shown in Table 3. All these descriptors were calculated with the +QSAR module in Cerius2.[20]

Statistical Analysis. The stepwise multiple linear regression method was used to identify the most contributing variables to a $t_{1/2}$ value among the 30 chemical descriptors defined above. This regression method is especially useful when the number of variables is large and when the key descriptors are not known in advance. It begins with an equation containing only a single variable and involves adding variables sequentially. The F value controls whether a variable will be added to or deleted from the equation. The F value is the ratio of the explained variance to the residual variance. The variable with the largest F value greater than the specified value is added first. Additionally, variables are added during subsequent steps. Likewise, if the F value of a variable falls below a specified value, the variable is removed. In this study, the value of 4.00 was used as the control F value, which is recommended by the +QSAR module in Cerius2.[20]

RESULTS

Cassette versus Individual Dosing. To confirm the reliability of the data obtained by the cassette dosing method, we compared the PK parameters obtained by the cassette dosing method and those obtained by the ordinary individual dosing method. Plasma concentration versus time profiles

Table 1. Chemical Structures and Observed Three PK Parameters in the First Series

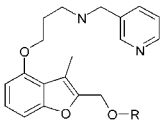

1 - 60

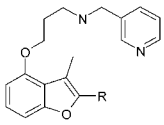

61 - 83

no.	-R	ln($t_{1/2}$)	ln(Cl)	ln(V_{ss})					
1	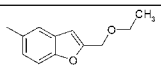	-0.386	2.104	1.946	27		0.432	1.131	1.841
2		-0.274	2.208	2.079	28		0.621	1.194	1.960
3	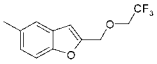	0.501	2.241	2.901	29		1.008	1.099	2.282
4	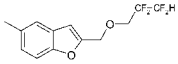	0.663	2.219	2.986	30		0.476	1.723	2.407
5	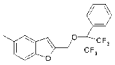	1.188	-0.105	1.099	31		0.647	1.825	2.639
6	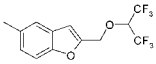	2.126	0.916	3.040	32		0.673	1.569	2.416
7	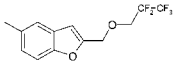	2.454	0.470	3.016	33		0.779	1.194	2.067
8	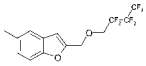	2.518	0.262	2.827	34		-0.994	1.548	0.833
9	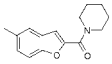	0.293	1.194	1.482	35		0.166	1.758	1.946
10		0.445	1.428	1.988	36	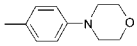	0.451	1.224	1.825
11		0.732	1.739	2.674	37	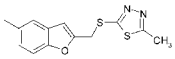	0.438	1.459	2.104
12	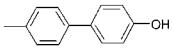	0.432	1.607	2.186	38		0.140	1.435	1.609
13		-0.844	1.482	0.693	39		-0.329	1.740	1.649
14		0.637	1.030	1.887	40		0.451	1.482	2.197
15	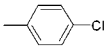	0.888	1.668	2.760	41		-0.528	1.917	1.629
16	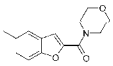	-0.020	1.435	1.386	42		-0.713	2.186	1.459
17	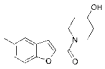	0.779	0.336	0.788	43		0.385	2.015	2.542
18	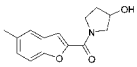	0.086	1.686	1.775	44		0.351	1.740	2.054
19	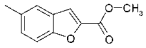	0.174	1.841	2.104	45	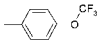	1.026	1.705	2.970
20	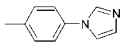	0.470	1.482	1.902	46		0.039	1.668	1.808
21		0.457	1.131	1.723	47		-0.755	1.917	1.482
22		0.392	1.548	2.140	48		1.001	1.705	2.960
23		0.631	1.589	2.351	49	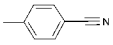	0.182	1.705	1.988
24		0.239	1.281	1.705	50	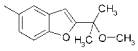	-0.478	2.688	2.380
25		0.975	1.887	3.020	51	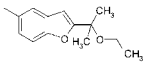	-0.400	2.646	2.342
26		0.548	1.504	2.175	52		-0.942	1.224	0.642
					53		-0.821	1.723	1.253

Table 1 (Continued)

no.	-R	ln($t_{1/2}$)	ln(Cl)	ln(V_{ss})					
54		-0.994	1.668	0.956	69	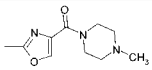	1.040	2.361	3.381
55		-0.942	1.629	1.065	70	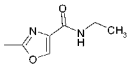	-0.777	1.435	0.642
56	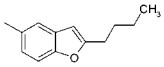	-0.186	2.370	2.175	71	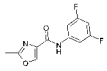	1.054	1.872	3.077
57	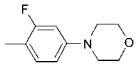	0.255	1.841	1.946	72		-1.309	1.253	0.000
58		1.273	1.548	2.785	73	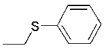	0.315	1.526	1.988
59		0.507	1.887	2.434	74	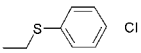	0.525	1.792	2.549
60	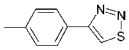	-0.598	1.917	1.629	75		0.837	2.219	3.096
61		0.300	2.595	3.096	76		-0.616	2.186	1.758
62		0.501	2.632	3.453	77	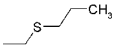	0.131	1.758	1.902
63		0.495	1.887	2.617	78		-1.022	1.856	1.030
64	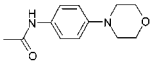	-0.211	1.825	1.629	79	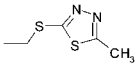	-0.580	1.335	0.993
65		-0.248	2.015	1.917	80		-0.151	3.068	3.045
66	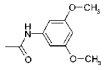	0.122	1.974	2.186	81	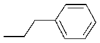	0.122	1.841	2.175
67		-0.083	1.902	1.988	82		1.250	1.131	2.653
68	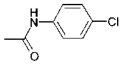	0.663	1.902	2.747	83		-0.777	1.386	0.588

of the five compounds in the individual and cassette dosing methods are plotted in Figure 2. The shapes of the plasma concentration−time profiles in cassette dosing were very similar to those in individual dosing. The ratios of five PK parameters between cassette and individual dosing methods (cassette/individual) were calculated. The mean ratios of $C_{10\text{min}}$, AUC, Cl, V_{ss}, and $t_{1/2}$ values were 1.12, 1.24, 0.81, 0.99, and 1.32, respectively. The result indicated that PK parameters derived from the cassette dosing method were comparable to those from the individual dosing method and these PK parameters could be used for the QSPKR study.

Furthermore, the variations of PK parameters of the reference compound (**1**) in 44 cassette dosing experiments were compared to show the stability of the cassette dosing method. As one example, the $t_{1/2}$ values of the reference compound in the cassette dosing experiments are plotted in Figure 3. The mean $t_{1/2}$ value was 1.28 h. Approximately 2-fold longer half-lives were observed in only three cases (experiment nos. 8, 22, and 40). The value of overall variation excluding these three cases was 28%. From this examination, it was found that the variation of the $t_{1/2}$ values was small in the overall cassette dosing experiments. The variations of other PK parameters ($C_{10\text{ min}}$, AUC, Cl, and V_{ss}) were also acceptable based on standard deviation limits.

QSPKR Analysis for First and Second Series. Initially, we analyzed the first series of the compounds consisting of ether and amide derivatives shown in Table 1. The stepwise multiple linear regression analysis with 30 chemical descriptors gave a good QSPKR equation with four variables.

$$\ln(t_{1/2}) = 0.009\cdot\text{PNSA}(75.44) - 0.212\cdot\text{Rotlbonds}(9.31) + 0.003\cdot\text{SASA}(5.92) - 0.296\cdot\text{HBD}(4.99) - 1.444 \quad (n = 83,\ r = 0.784,\ q = 0.744) \quad (1)$$

In eq 1, the numbers in parentheses are the F value of each variable, n is the number of data points in deriving the equation, r is the correlation coefficient, and q is the cross-validated version of the correlation coefficient derived from the leave-one-out (LOO) procedure. In LOO, one sample in the data set is omitted, and the rederived QSPKR model is used to predict the target PK property of the omitted sample. This process is repeated until the target PK property of all samples in the data set has been predicted once. The plot of the observed versus calculated $t_{1/2}$ values is shown in Figure 4.

In the second stage, the $t_{1/2}$ values of ketone derivatives shown in Table 2 were predicted by eq 1 and performance

Table 2. Chemical Structures and Observed Three PK Parameters in the Second Series

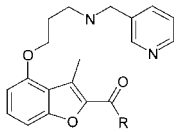

84 - 107

no.	-R	ln($t_{1/2}$)	ln(Cl)	ln(V_{ss})
84		-0.616	1.569	0.470
85		-0.799	1.308	0.405
86		-0.528	1.411	1.131
87		-0.580	1.609	1.099
88		-0.821	1.308	0.642
89		-0.713	1.569	0.788
90	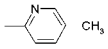	-0.545	1.459	0.993
91		-0.654	1.548	0.875
92	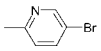	-0.094	2.322	2.425
93		-0.223	1.224	1.224
94		-0.236	0.916	0.916
95		-0.211	1.411	1.308
96		-1.079	1.335	0.405
97		-0.673	1.281	0.742
98		-0.916	1.253	0.531
99		-0.151	0.875	0.916
100		-0.777	1.609	0.693
101		-0.431	1.686	1.435
102		0.182	1.030	1.386
103		-0.117	1.435	1.459
104		-0.755	1.099	0.588
105		-0.916	1.224	0.470
106		-0.968	2.128	1.163
107		-0.799	1.548	0.742

Table 3. List of Chemical Descriptors Used in SQPKR Study

no.	descriptor	symbol
1	sum of atomic polarizabilities	Apol
2	magnitude of dipole moment	Dipole
3	dipole moment in *x* direction	Dipole_x
4	dipole moment in *y* direction	Dipole_y
5	dipole moment in *z* direction	Dipole_z
6	highest occupied molecular orbital energy	HOMO
7	lowest unoccupied molecular orbital energy	LUMO
8	radius of gyration	RadOfGyration
9	total molecular solvent-accessible surface area	SASA
10	partial positive surface area	PPSA
11	partial negative surface area	PNSA
12	difference in charged partial surface area	DPSA
13	molecular surface area	Area
14	magnitude of principal moment of inertia	PMI
15	principal moment of inertia in *x* direction	PMI_x
16	principal moment of inertia in *y* direction	PMI_y
17	principal moment of inertia in *z* direction	PMI_z
18	molecular volume	Vm
19	number of rotatable bonds	Rotlbonds
20	number of hydrogen bond acceptors	HBA
21	number of hydrogen bond donors	HBD
22	atomic-based octanol/water partitiion coefficient	AlogP
23	desolvation free energy for water	Fh2o
24	desolvation free energy for octanol	Foct
25	molecular refractivity	MolRef
26	order zero chi index	CHI-0
27	order one chi index	CHI-1
28	order two chi index	CHI-2
29	order of three chi index (type 1)	CHI−3_P
30	order of three chi index (type 2)	CHI−3_C

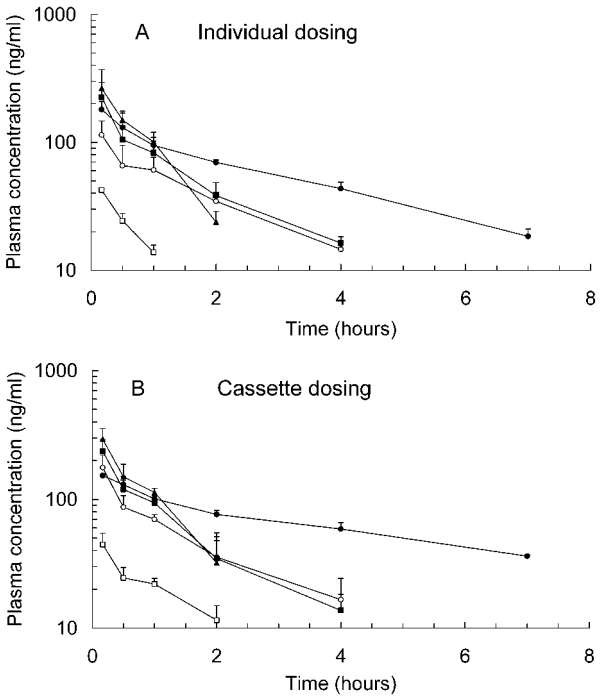

Figure 2. Plasma concentration versus time profiles of five compounds from individual (A) and cassette (B) dosing studies. Data are mean of three rats.

of the model was examined. Figure 5 is the plot of the observed versus predicted $t_{1/2}$ values. The predicted values of ketone derivatives are overestimated compared to those of ether derivatives. Moreover, the two regression lines, indicated by A and B, are of identical slope and the deviation between the two lines would be a constant. This indicated that the ketone data set could merge with the data set of the ether and amide derivatives if an indicator variable was used.

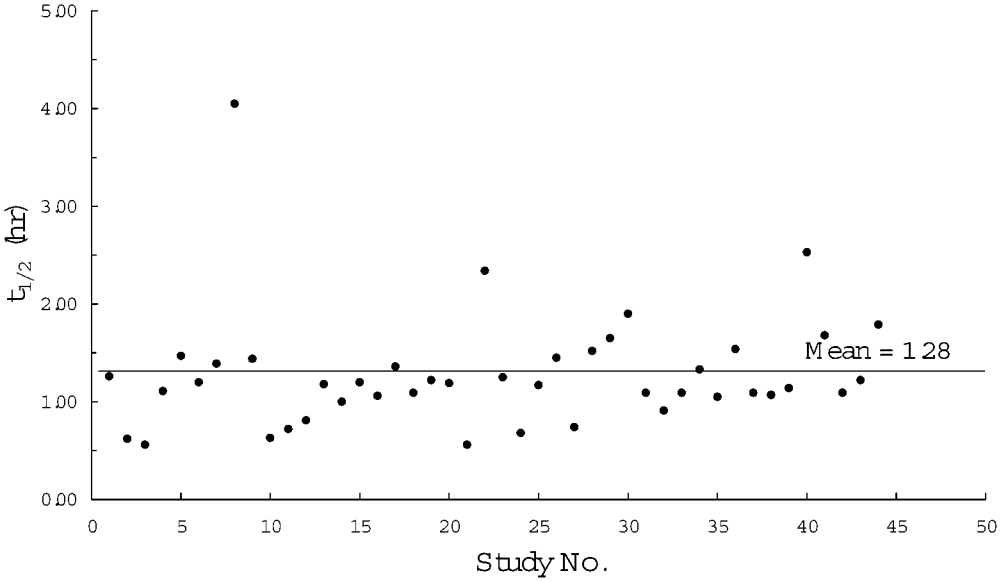

Figure 3. Variation of $t_{1/2}$ values of the reference compound (**1**) in 44 cassette dosing experiments. Data are mean of three rats.

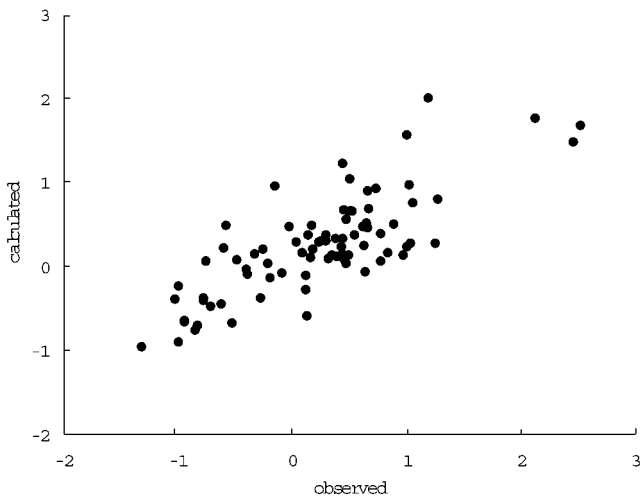

Figure 4. Plot of observed versus calculated $t_{1/2}$ values from eq 1.

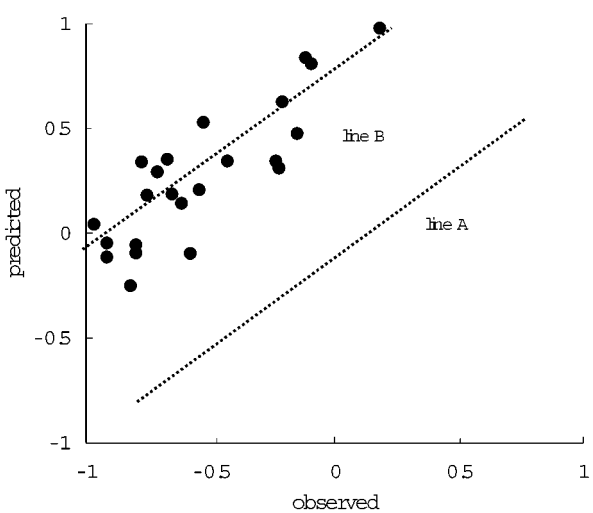

Figure 5. Plot of observed versus predicted $t_{1/2}$ values from eq 2. In the figure, lines A and B represent the regression slopes for the first and second series, respectively.

The whole data set was subjected to multiple linear regression analysis with the same descriptors as in eq 1.

$$\ln(t_{1/2}) = 0.009\cdot\text{PNSA}(97.21) - 0.206\cdot\text{Rotlbonds}(15.11) + 0.003\cdot\text{SASA}(7.99) - 0.295\cdot\text{HBD}(6.06) - 0.732\cdot\text{I_ketone}(50.13) - 1.424 \quad (n = 107,\ r = 0.831,\ q = 0.804) \quad (2)$$

The significant QSPKR model was obtained when the indicator variable (I_ketone) was used. In eq 2, the indicator variable has the values of 1 and 0 for the ketone (Table 2) and nonketone derivatives (Table 1), respectively. The indicator variable has no effect on the regression line for the nonketone derivatives. However, for the ketone derivatives, this has the effect of subtracting a constant (approximately 0.7 in log range) from all the $t_{1/2}$ values.

QSPKR Analysis for Whole Data Set. As I_ketone is an indicator variable with only mathematical meaning, we tried to replace it with a more significant chemical descriptor. Among the 26 remaining chemical descriptors other than the four descriptors used in eq 2, AlogP was found to be most suitable based on the high correlation with I_ketone (0.552). The replacement of I_ketone by AlogP gave eq 3.

$$\ln(t_{1/2}) = 0.009\cdot\text{PNSA}(103.61) - 0.177\cdot\text{Rotlbonds}(19.46) + 0.002\cdot\text{SASA}(3.47) - 0.022\cdot\text{HBD}(0.07) + 0.164\cdot\text{AlogP}(27.43) - 2.316 \quad (n = 107,\ r = 0.813,\ q = 0.776) \quad (3)$$

The *F* statistic values of SASA and HBD indicate that they are no longer significant. Moreover, the predicted $t_{1/2}$ values of two compounds (**5** and **69**) largely deviated from the experimental values, though the reason is not clear from their chemical structures alone. Removal of these two variables and these compounds resulted in eq 4, which is very similar to eq 3.

$$\ln(t_{1/2}) = 0.011\cdot\text{PNSA}(157.04) + 0.198\cdot\text{AlogP}(63.09) - 0.081\cdot\text{Rotlbonds}(6.57) - 2.330 \quad (n = 105,\ r = 0.843,\ q = 0.827) \quad (4)$$

The correlation matrix between the key variables associated with eq 4 were as follows: PNSA versus AlogP, 0.063;

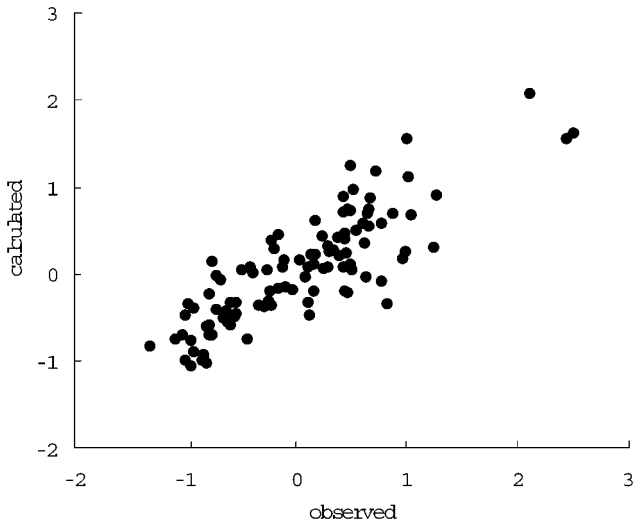

Figure 6. Plot of observed versus calculated $t_{1/2}$ values from eq 4.

PNSA versus Rotlbonds 0.474; AlogP versus Rotlbonds, 0.055. The variables were reasonably orthogonal although there was a weak collinearity between PNSA and Rotlbonds. From the good statistical performance and simplicity, we concluded that eq 4 was the final QSPKR model that explained the $t_{1/2}$ values for the whole data set.[21] The plot of the observed versus calculated $t_{1/2}$ values is shown in Figure 6.

DISCUSSION

Similar plasma concentration−time profiles and PK parameters were obtained in cassette and individual dosing methods with intravenous administration of five compounds in rats (Figure 2). A slight increase of $t_{1/2}$ value was observed in cassette dosing compared to those in individual dosing (the value of mean ratios was 1.32). This result suggested that the minimum drug−drug interaction could be occurring in cassette dosing. However, the difference of $t_{1/2}$ values is only 30%. Such an increase seems to be insignificant and acceptable for this QSPKR analysis. Similar experimental errors have been also reported by other groups.[3−5] Furthermore, variation of PK parameters of the reference compound (**1**) in the 44 cassette dosing experiments was small except for three cases (Figure 3). Hence, the cassette dosing approach is acceptable in evaluating new chemical entities at the early stage in drug discovery.

Since the final QSPKR model is reliable and simple, it is useful to interpret the model for designing new derivatives having an appropriate $t_{1/2}$ value. The most important factor influencing the model is PNSA according to the F value. PNSA means the sum of the solvent-accessible surface areas of negatively charged atoms such as oxygen, nitrogen, and halogen atoms. The model means that PNSA should be kept to a maximum value by introducing negatively charged groups to the terminal part of a chain at the C-2 position. From the significant descriptor "PNSA", new Nmt inhibitors can be designed by adding halogen atoms such as F atoms to the terminal part. It is widely known that the oxidation of benzylic and allylic positions by cytochrome P450 (especially CYP3A4) can be blocked by the introduction of halogen atoms.[22] The negatively charged substituents lead to a small hepatic clearance (Cl) and then a long $t_{1/2}$ value. The high lipophilicity (AlogP) of the compound is an advantage for long $t_{1/2}$ because it leads to a high distribution volume (V_{ss}). The positive relationship between lipophilicity and the distribution volume has been observed and reported in an early QSPKR study.[23] Fewer rotational bonds (Rotlbonds) are also beneficial for the compound to remain in the plasma. One interpretation of this property is that a compound with many rotational bonds has more chances to react with other molecules. Thus, it is probable that such a compound is metabolized by several enzymes.

SUMMARY

In summary, the cassette dosing PK study was useful in measuring the PK properties of our Nmt inhibitors in a high-throughput manner. The multivariate statistical approach was useful in interpreting the relationships between the $t_{1/2}$ values and the chemical structures. The model would be useful to predict $t_{1/2}$ values of the inhibitors and hence helpful in designing new inhibitors having a long half-life value. In general, it is desirable to improve many parameters such as pharmacological activity, PK parameters, and safety indices simultaneously in order to develop a good medicine. Good mathematical models that predict such properties will be indispensable to achieve multidimensional optimization. The combination of high-throughput PK measurements and the multivariate statistical approach is one of the ways to establish such mathematical models efficiently.

REFERENCES AND NOTES

(1) Tarbit, M. H.; Berman, J. High-throughput approaches for evaluating absorption, distribution, metabolism and excretion properties of lead compounds. *Curr. Opin. Chem. Biol.* **1998**, *2*, 411−416.
(2) Watt, A. P.; Morrison, D.; Evans, D. C. Approaches to higher-throughput pharmacokinetics (HTPK) in drug discovery. *Drug Discovery Today* **2000**, *5*, 17−24.
(3) Berman, J.; Halm, K.; Adkison, K.; Shaffer, J. Simultaneous Pharmacokinetic Screening of a Mixture of Compounds in the Dog Using API LC/MS/MS Analysis for Increased Throuput. *J. Med. Chem.* **1997**, *40*, 827−829.
(4) Shaffer, J. E.; Kimberly, K.; Adkison, K.; Halm, K.; Hedeen, K.; Berman, J. Use of "N-in-One" Dosing to Create an in Vivo Pharmacokinetics Database for Use in Developing Structure-Pharmacokinetic Relationships. *J. Pharm. Sci.* **1999**, *88*, 313−318.
(5) Frick, L. W.; Adkison, K. K.; Wells-Knecht, K. J.; Woollard, P.; Higton, D. M. Cassette dosing: rapid in vivo assessment of pharmacokinetics. *Pharm. Sci. Technol. Today* **1998**, *1*, 12−18.
(6) Olah, T. O.; Mcloughlin, D. A.; Gilbert, J. D. The simultaneous Determination of Mixtures of Drug Candidates by Liquid Chromatography/Atmospheric Pressure Chemical Ionization Mass Spectrometry as *In Vivo* Drug Screening Procedure. *Rapid Commun. Mass Spectrom.* **1997**, *11*, 17−23.
(7) Bayliss, M. K.; Frick, L. W. High-throughput pharmacokinetics: Cassette dosing. *Curr. Opin. Drug Discovery Dev.* **1999**, *2*, 20−25.
(8) Beaudry, F.; Yves Le Blanc, J. C.; Coutu, M.; Brown, N. K. In Vivo Pharmacokinetic Screening in Cassette Dosing Experiments: the Use of On-Line Prospekt Liquid Chromatography/Atmospheric Pressure Chemical Ionization Tandem Mass Spectrometry Technology in Drug Discovery. *Rapid Commun. Mass Spectrom.* **1998**, *12*, 1216−1222.
(9) Allen, M. C.; Shah, T. S.; Day, W. W. Rapid Determination of Oral Pharmacokinetics and Plasma Free Fraction Using Cocktail Approaches: Methods and Application. *Pharm. Res.* **1998**, *15*, 93−97.
(10) Cox, K. A.; Dunn-Meynell, K.; Korfmacher, W. A.; Broske, L.; Nomeir, A. A.; Lin, C.; Cayen, M. N.; Barr, W. H. Novel *in vivo* procedure for rapid pharmacokinetic screening of discovery compounds in rats. *Drug Discovery Today* **1999**, *4*, 232−237.
(11) Hop, C. E. C. A.; Wang, Z.; Chen, Q.; Kwei, G. Plasma-Pooling Methods To Increase Throughput for in Vivo Pharmacokinetic Screening. *J. Pharm. Sci.* **1998**, *87*, 901−903.
(12) Kuo, B.-S.; Noord, T.; Feng, M.; Wright, D. Sample pooling to expedite bioanalysis and pharmacokinetic research. *J. Pharm. Biomed. Anal.* **1999**, *20*, 39−47.

(13) Toon, S.; Rowland, M. Structure-pharmacokinetic relationships among the barbiturates in the rat. *J. Pharmacol. Exp. Ther.* **1983**, *225*, 752−763.
(14) Mayer, J. M.; van de Waterbeemd, H. Development of quantitative structure-pharmacokinetic relationships. *Environ. Health Perspect.* **1985**, *61*, 295−306.
(15) Gobburu, J. V. S.; Shelver, W. H. Quantitative structure-pharmacokinetic relationships (QSPR) of beta blockers derived using neural networks. *J. Pharm. Sci.* **1995**, *84*, 862−865.
(16) Herman, R. A.; Veng-Pedersen, P. Quantitative structure-pharmacokinetic relationships for systemic drug distribution kinetics not confined to a congeneric series. *J. Pharm. Sci.* **1994**, *83*, 423−428.
(17) Van der Graaf, P. H.; Nilsson, J.; Van Schaick, E. A.; Danhof, M. Multivariate Quantitative Structure-Pharmacokinetic Relationships (QSPKR) Analysis of Adenosine A_1 Receptor Agonists in Rat. *J. Pharm. Sci.* **1999**, *88*, 306−312.
(18) Maubuchi, M.; et al. *Bioorg. Med. Chem. Lett.* **2001**, *11*, 1833−1837.
(19) Ebiike, H.; et al. Submitted for publication in *Bioorg. Med. Chem. Lett.*
(20) *Cerius2*, version 4.0; Molecular Simulations Inc.: San Diego, USA.
(21) For reference, we made the stepwise analysis on the full data set.

$$\ln(t_{1/2}) = 0.009\cdot\mathrm{PNSA}(66.48) + 0.168\cdot\mathrm{AlogP}(39.92) - 0.193\cdot\mathrm{Rotlbonds}(14.51) + 0.001\cdot\mathrm{PMI_x}(7.69) - 1.091 \quad (n = 105,\ r = 0.855,\ q = 0.836)$$

The equation has the same descriptors as eq 4 except for an additional PMI_x. Because of simplicity and similar statistical quality, eq 4 was chosen for the final model.
(22) Van de Waterbeemd, H.; Smith, D. A.; Beaumont, K.; Walker, D. K. Property-Based Design: Optimization of Drug Absorption and Pharmacokinetics. *J. Med. Chem.* **2001**, *44*, 1−21.
(23) Seydel, J. K.; Trettin, D.; Cordes, H. P. Quantitative Structure-Pharmacokinetic Relationships Derived on Antibacterial Sulfonamides in Rats and Its Comparison to Quantitative Structure−Activity Relationships. *J. Med. Chem.* **1980**, *23*, 607−613.

CI0102517